The speckle-free nature of photoacoustic imaging

Zijian Guo, Li Li, Lihong V. Wang

Zijian Guo, Li Li, Lihong V. Wang, "The speckle-free nature of photoacoustic imaging," Proc. SPIE 7177, Photons Plus Ultrasound: Imaging and Sensing 2009, 71772J (24 February 2009); doi: 10.1117/12.809374

SPIE.

Event: SPIE BiOS, 2009, San Jose, California, United States

The speckle-free nature of photoacoustic tomography

Zijian Guo*, Li Li* and Lihong V. Wang†

Optical Imaging Laboratory, Department of Biomedical Engineering, Washington University
1 Brookings Drive, Saint Louis, Missouri 63130, USA

ABSTRACT

Photoacoustic imaging for biomedical applications has seen significant growth during the past few years. Despite its coherent nature, it possesses a unique advantage to produce images devoid of speckle artifacts. The reason responsible for this salient feature has not been addressed so far. We found this is a direct result of its extraordinary absorption contrast. Our discovery is explained using simulations based on a practical photoacoustic imaging system.

Keywords: Speckle, photoacoustic imaging

1. INTRODUCTION

Speckle is considered a ubiquitous physical phenomenon existing in all coherent imaging modalities, such as laser imagery [1,2], ultrasonography [3,4], synthetic aperture radar [5], and optical coherence tomography [6]. It is formed by the mutual-interference between waves − either scattered from randomly distributed scatterers, or reflected by different parts of a rough surface − whose phases have been completely randomized. The speckle pattern generally has a chaotic granular appearance. Although this fluctuation usually has a non-vanishing contrast, it is not directly correlated to the real structure of sample. It reduces both the effective spatial resolution and the delectability of small lesions, thus deteriorates the image quality significantly. For decades, a lot of efforts have been made to relieve this undesirable deterioration through compounding different images or digital signal processing. However, they can only reduce the speckle artifacts to a limited extent, and the improvement is achieved inevitably at the cost of system complexity, imaging time or spatial resolution. In this letter, we explain the speckle free nature of a novel coherent imagery: photoacoustic imaging.

Although the photoacoustic effect was first reported by A. G. Bell in 1880, photoacoustic imaging is only recently emerging as a promising imaging technique for biomedical applications [7]. A unique distinction between photoacoustic imaging with aforementioned modalities is that it exploits the optical absorption contrast [8], instead of scattering. Because many physiologically important molecules, like hemoglobin, possess high characteristic absorption, photoacoustic imaging has provided images of vasculature and hemodynamic functions with outstanding quality *in vivo* [9,10]. More recently, the feasibility of visualizing specific molecular-related events by photoacoustic imaging has also been demonstrated [11]. In photoacoustic imaging, the tissue is usually irradiated by a short-pulsed laser. Locally absorbed light is converted into heat, which is further converted to a pressure rise via thermoelastic expansion. The initial pressure rise then propagates as an ultrasonic wave − photoacoustic wave, which is detected by ultrasonic transducers. An image is then formed from signals recorded at different locations surrounding the tissue. Since ultrasound scattering is 2-3 orders of magnitude weaker than optical scattering in biological tissues, photoacoustic imaging can achieves a much better spatial resolution than traditional optical modalities beyond the optical ballistic regime (depth >1 mm).

Curiously enough, investigators have also noticed that photoacoustic method produces images devoid of speckle artifacts, despite its coherent nature [8]. The reason responsible for this unique advantage has not been addressed. We found this is closely related to nature of the absorption contrast. In photoacoustic imaging, the initial pressure rise induced as a result of local absorption is all positive. By comparison, in ultrasound imaging, a typical scattering-based modality, the scattered acoustic waves usually have completely randomized phase between 0 and 2π, i.e., both positive and negative polarities, depending on the size, shape and acoustic impedance of the scatterers.

* These authors contributed equally.
† Corresponding author. Email: lhwang@biomed.wustl.edu

Photons Plus Ultrasound: Imaging and Sensing 2009, edited by Alexander A. Oraevsky, Lihong V. Wang,
Proc. of SPIE Vol. 7177, 71772J · © 2009 SPIE · CCC code: 1605-7422/09/$18 · doi: 10.1117/12.809374

2. SIMULATION METHODS AND RESULTS

We explain our finding based on simulation. Currently, photoacoustic imaging has two major forms of implementation. One resembles B-mode ultrasound. Photoacoustic signals are collected by a scanning-focused ultrasonic transducer. An image is formed by properly aligning these measurements [9]. The other is similar to X-ray computed tomography (CT). It is based on an array of unfocused ultrasonic transducers placed surround the object. Image is made by a reconstruction algorithm [8]. Our following simulation is based on a reflection-mode photoacoustic imaging system developed in our laboratory [12], which allows deep penetration up to several centimeters in tissue. This system utilizes a broadband ultrasonic transducer with center frequency at 5 MHz. A photoacoustic depth profiling of tissue's absorbing structure is achieved at each lateral location. A cross-sectional or volumetric image is composed by aligning multiple measurements at their correct lateral positions. It belongs to the first category. However, the principle discussed here remains true for all photoacoustic implementations given the linearity of the systems.

A real absorbing structure (e.g. blood in a blood vessel) can be modeled as a collection of randomly distributed absorbers (e.g. red blood cells). The absorbers are usually so densely packed that we cannot resolve individual absorbers. For example, a normal adult has about 5 million erythrocytes (mainly red blood cells) per microliter of blood. The axial resolution of the targeted system, which is limited by the transducer's bandwidth, is measured ~144 μm, while the lateral resolution is determined by width of the focal zone, which is ~560 μm. Thus, when imaging blood vessels, the transducer receives photoacoustic waves at any instant from ~5.8×10^4 absorbers, which interfere with each other.

For simplification, we first simulated a 1-D problem. Our numerical phantom contained a front boundary of an absorbing structure. The absorbing structure is composed by randomly distributing a large number of absorbers along the axial direction of the transducer, and the front boundary is located at 0.5 mm from the transducer surface. The exact boundary positions are plotted as dotted lines. The absorption coefficients of these absorbers followed a normal distribution. The photoacoustic wave was assumed to be excited by a delta laser pulse. The optical attenuation was neglected, since it was not the key factor in our explanation. In Fig. 1, the simulated photoacoustic profiling of the 1-D phantom are compared with ultrasound imaging of a phantom of the same geometry but including a scattering object. As a convention, the envelope of the acoustical signal is presented in images in order to present the magnitude of absorption or scattering. Thus, in Fig. 1, the envelope was also obtained through Hilbert transform and plotted as dashed lines.

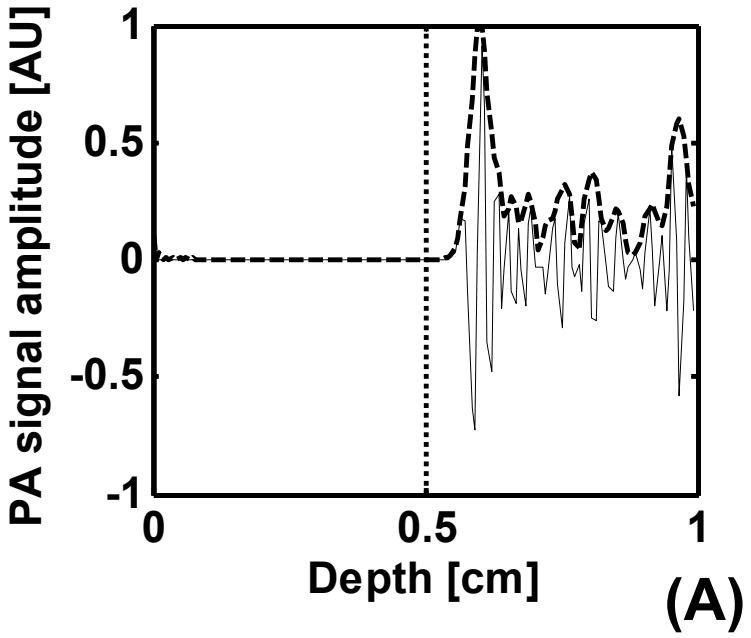

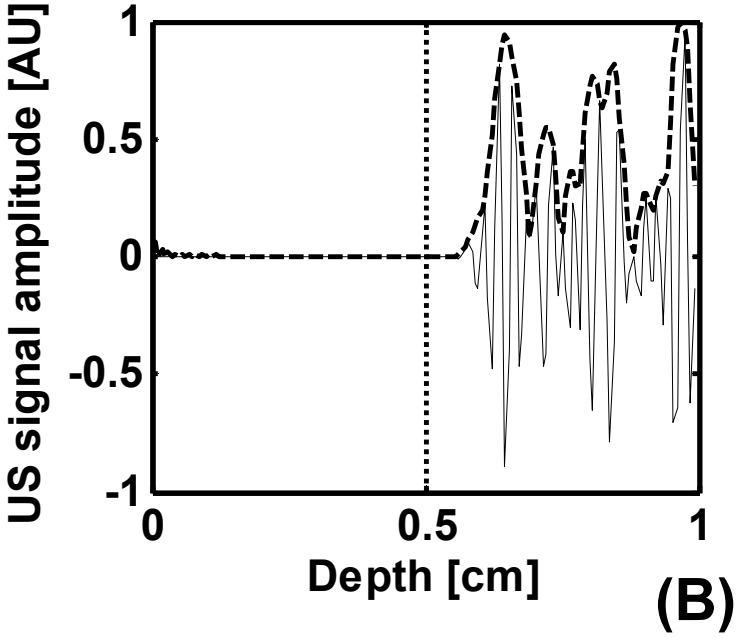

(B)

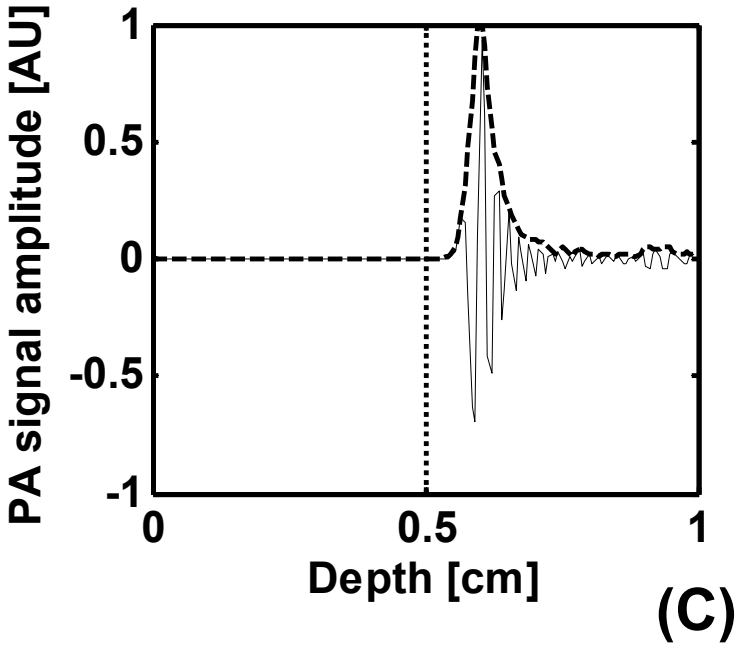

(C)

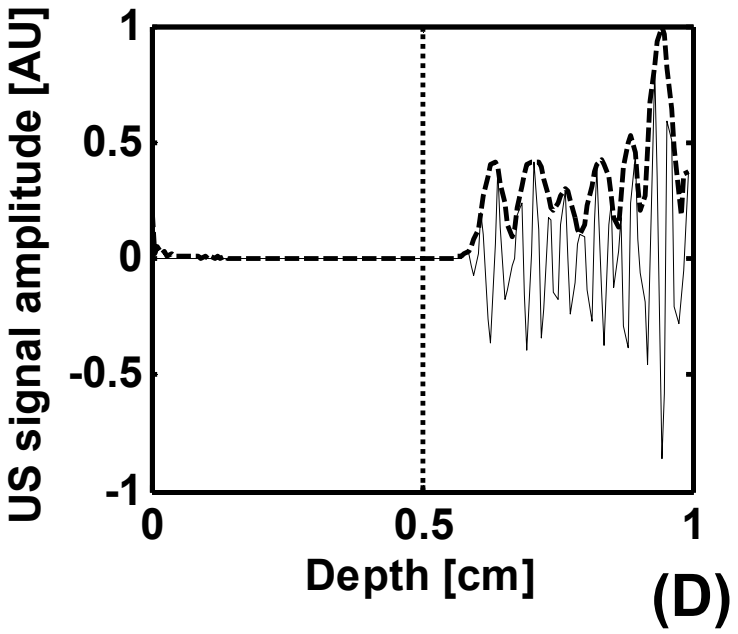

Figure 1. **Simulated depth profiles of 1-D object.** (A) Photoacoustic imaging, absorber density: 1,000/ λ; (B) Ultrasound imaging, scatterer density: 1,000/λ; (C) Photoacoustic imaging, absorber density: 100,000/ λ; (D) Ultrasound imaging, scatterer density: 100,000/ λ. λ: the wavelength of 5-MHz ultrasound in tissue.

In Figs. 1(A) and (B), the object has the same particle density. By comparison of the two, we first notice prominent semi-deterministic boundaries, which dominate the random speckle-like fluctuations in the middle, presented in photoacoustic images. On the contrary, the speckled fluctuations in the ultrasound images spread across the whole object without outstanding boundaries. As stated above, the speckle is formed by mutual-interference of coherent waves with completely randomized phases. Two components contribute to the phase difference between waves, which reach transducer at the same time: the different time-of-flight and the initial phase after excitation. When profiling the smooth central part of the object in both photoacoustic and ultrasound imaging, we always receive acoustic waves from particles with completely randomized phase, which can be achieved only by the time-of-flight difference. However, particles, close to the objects' edge or located within a prominent local feature, give out waves that reach the transducer after roughly identical time-of-flight. Here, the initial excitation phase plays a key role. The initial photoacoustic pressure, generated right after the pulsed laser illumination, is always positive and in phase. Thus waves add constructively to manifest boundaries. To the opposite, the scattered ultrasonic waves from particles, with different sizes, shapes, acoustic and mechanical properties, usually possess initial phases ranging randomly from 0 to 2π. As a result, the speckle pattern dominates almost everywhere.

The contrast of the fluctuation, defined as the ratio of the standard deviation of speckle-like fluctuation in the middle over the peak signal and representing the visibility of this unwanted fluctuation, was also found to decrease with increase of absorber density [Fig. 1(A) and Fig 1(C)]. We quantified this relationship in Fig. 2, and found the slope of the linear fitting between the logarithms of fluctuation contrast and the absorber density was close to 0.5. This implied an inverse square-root dependence, which we should expect as a natural result of the central limit theory. On the contrary, the contrast of speckle keeps almost constant in ultrasound imaging [Fig. 1(B) and Fig 1(D)].

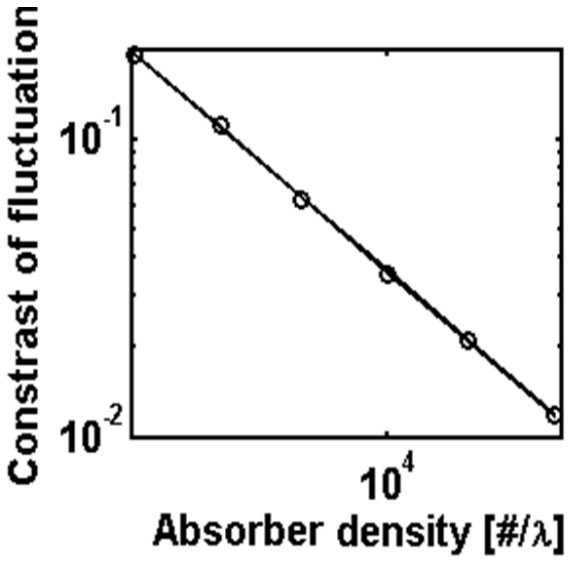

Fig. 2. **Relation between contrast of fluctuation and the absorber density.** Circle: calculation based on 10 simulations for each absorber density; Solid line: linear fitting.

We simulated more realistic situations. Photoacoustic cross-sectional images of tissue slabs, which were filled with absorbers with a physiological density of 5 million/μl, were obtained under full 3-D geometry. For a slab with a thickness of 2 mm [Fig. 3 (A)], we observed strong signal accumulation at the top and bottom boundary. The simulation result matches our experimental experiences well. Figure 3 (B) shows ultrasonic B-scan of a scattering structure with same geometry. The boundary buildup disappeared and the speckle dominates everywhere.

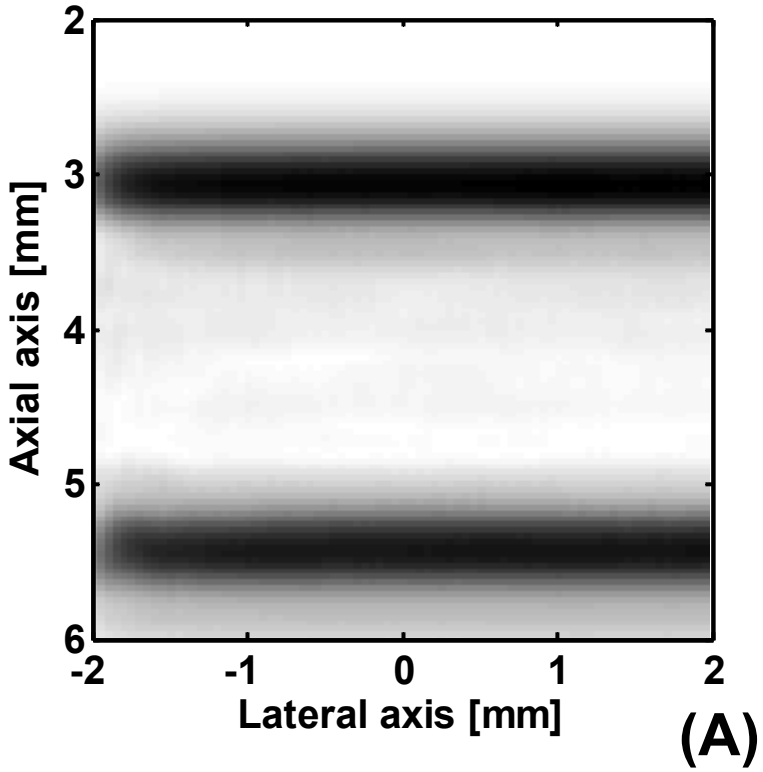

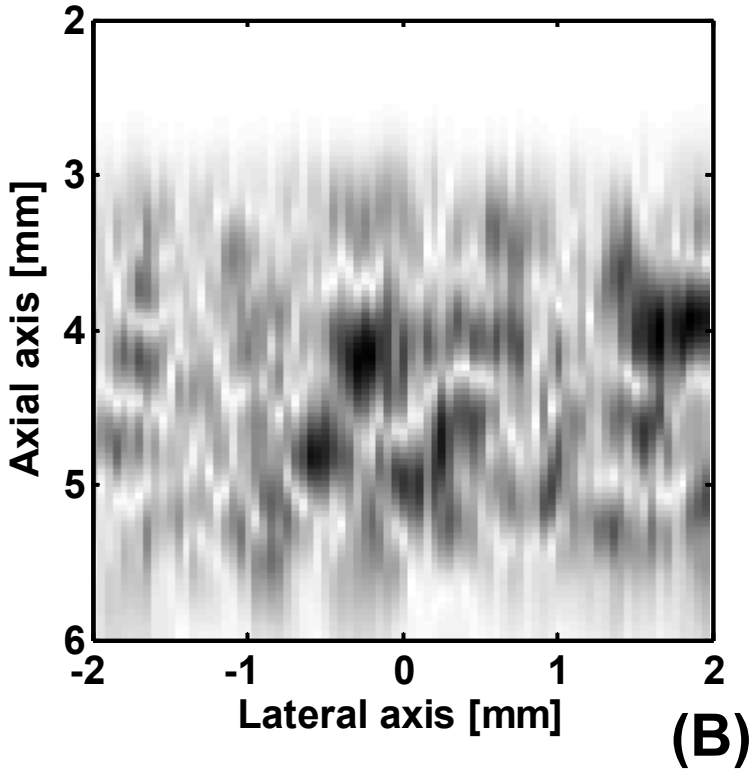

Fig. 3. **Simulated cross-sectional photoacoustic and ultrasonic images of a slab.**

3. CONCLUTION

In summary, we explained that the lack of speckle in photoacoustic imaging due to all positive initial photoacoustic pressure rise. The prominent boundary or local features usually show up as dominant features in photoacoustic images due to constructive interference. As a result, the contrast of the speckle-like fluctuation decreases with the increase of absorbers' density. This is a unique advantage of imaging techniques based on absorption contrast.

ACKNOWLEDGMENTS

We would like to thank Meng-Lin Li, Minghua Xu and Roger Zemp for useful discussion. This research is funded in part by the National Institutes of Health under Grant No. R01 NS46214 (BRP) and R01 EB000712.

REFERENCES

1. Dainty, J. C., *Laser Speckle and Related Phenomena* (Springer-Verlag, Berlin and New York, 1975).
2. Goodman, J. W.*, Speckle Phenomena in Optics: Theory and Applications* (Roberts & Company, Englewood, 2007).
3. Burckhardt, C. B., "Speckle in Ultrasound B-Mode Scans," IEEE Transactions on Sonics and Ultrasonics **25**, 1-6 (1978).
4. Wagner, R. F., Smith, S. W., Sandrik, J. M., and Lopez, H., "Statistics of Speckle in Ultrasound B-Scans," IEEE Transactions on Sonics and Ultrasonics **30**, 156-163 (1983).
5. Lee, J. S., "Speckle Suppression and Analysis for Synthetic Aperture Radar Images," Optical Engineering **25**, 636-643 (1986).
6. Schmitt, J. M., Xiang, S. H., and Yung, K. M., "Speckle in Optical Coherence Tomography," Journal of Biomedical Optics **4**, 95-105 (1999).
7. Xu, M., and Wang, L. V., "Photoacoustic imaging in biomedicine," Review of Scientific Instruments **77**, 041101 (2006).
8. Wang, L. V., "Tutorial on Photoacoustic Microscopy and Computed Tomography," IEEE Journal of Selected Topics in Quantum Electronics **14**, 171-179 (2008).
9. Wang, X., Pang, Y., Ku, G., Xie, X., Stoica, G., and Wang, L. V., "Non-invasive laser-induced photoacoustic tomography for structural and functional imaging of the brain in vivo," Nature Biotechnology **21**, 803-806 (2003).
10. Zhang, H. F., Maslov, K., Stoica, G., and Wang, L. V., "Functional photoacoustic microscopy for high-resolution and noninvasive in vivo imaging," Nature Biotechnology **24**, 848–851 (2006).
11. Li, L., Zemp, R., Lungu, G., Stoica, G., and Wang, L. V., "Photoacoustic imaging of lacZ gene expression *in vivo*," Journal of Biomedical Optics **12**, 020504 (2007).
12. Song, K., and Wang, L. V., "Deep reflection-mode photoacoustic imaging of biological tissue," Journal of Biomedical Optics **12**, 060503 (2007).